X-rays and accretion discs as probes of the strong gravity of black holes

A.C. Fabian

Institute of Astronomy, Madingley Road, Cambridge CB3 0HA, UK

Abstract. The observations and interpretation of broad iron lines in the X-ray spectra of Seyfert 1 galaxies are reviewed. The line profiles observed from MCG–6-30-15 and NGC 3516 show extended red wings to the line explained by large gravitational redshifts. The results are consistent with the emission expected from an X-ray irradiated flat accretion disc orbiting very close to a black hole. Results from XMM-Newton and Chandra are presented and the possibility of broad oxygen lines discussed.

INTRODUCTION

The optical (e.g. Ghez et al 2000; Eckart et al 1997; Gebhardt et al 2000; Ferrarese & Merritt 2000) and radio (e.g. Miyoshi et al 1995) evidence for compact central masses in the nuclei of many nearby galaxies is now very clear. The compact objects are consistent with being supermassive black holes. The data do not however probe the strong gravity regime of these holes, since the observed stars and gas orbit at more than 40,000 gravitational radii from the centre.

Much of the X-ray emission from accreting black holes should emerge from within a few 10s of gravitational radii. Aspects of this emission can provide us with a probe of the strong gravity of black holes. In particular the rapid variability, or in some cases quasi-periodic oscillations, and soft thermal emission from an accretion disc demonstrates the small size of the X-ray emission region.

Here I concentrate on the broad iron emission lines seen in the spectra of some Seyfert 1 galaxies. The line profile and its variability can reveal the geometry of the accretion flow, and strong gravitational effects, within a few gravitational radii of the black hole. The dominant expected line is that due to iron, as shown in Fig. 1 (George & Fabian 1991; Matt, Perola & Piro 1991). The spectrum shown is the result of a Monte-Carlo simulation of the emergent spectrum when a flat surface has been irradiated with a power-law X-ray spectrum. The gas is assumed to be neutral, although the important issue here is that the metals retain their K and L-shell electrons. The major emission line is iron K-α, due to its relatively high abudance (a cosmic mix is assumed) and high fluorescent yield (which increases as Z^4). Doppler broadening of this emission line, produced by the irradiation of

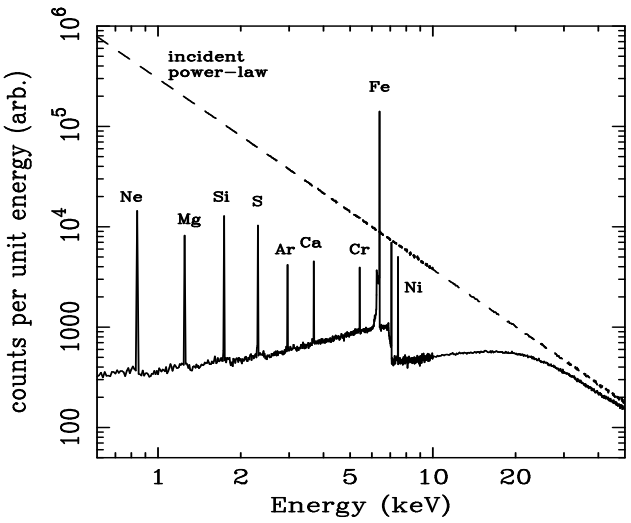

FIGURE 1. Monte Carlo simulation (by C. Reynolds) of the reflected continuum plus fluorescent line emission from a neutral slab of gas with comsic abundances. The incident power-law continuum is indicated by the dashed line. In practice the sum of the incident and reflected spectra are usually seen.

the surface of an accretion disc by hard X-rays from its corona, together with thr special relativistic effects of beaming and the transverse doppler effect and the general relativistic effect of gravitational redshift, lead to the observed profile being very broad and skew (Fabian et al 1989: Figs. 2, 3). The 'blue horn' of the line is most sensitive to the inclination angle of the disc (i.e. the importance of doppler broadening) and the 'red wing' is most sensitive to the inner radius (i.e. the gravitational redshift).

I OBSERVATIONS OF BROAD IRON LINES

A clear broad iron line was first seen with data from a 1994 ASCA observation of the Seyfert 1 galaxy MCG–6-30-15 (Tanaka et al 1995: Fig. 4). This was the result of a 4.5 day exposure on the source and is shown with the dominant power-law continuum removed. The data are well fit (Fabian et al 1995) by emission from an accretion disc stretching from about 6 gravitational radii (i.e. $6r_{\rm g} = 6GM/c^2$) to about 40 $r_{\rm g}$ and an inclination of about 30 deg. The surface emissivity falls as radius r^{-3}. A similar clear line has also been seen in NGC 3516 (Nandra et al 1999: Fig. 4). The shape of these lines is entirely consistent with the emitting region being a flat disc in Keplerian rotation close to a black hole.

K. Nandra (priv. comm.) has compiled the line spectra of several more Seyfert 1 galaxies (Fig. 5) which generally are weaker in flux, or have shorter exposures than

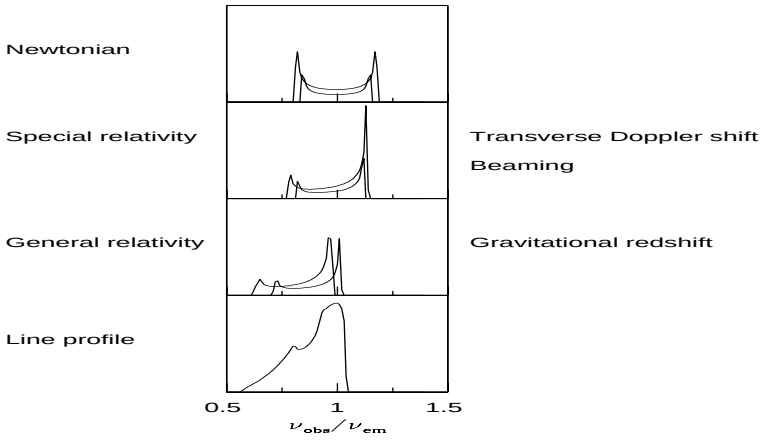

FIGURE 2. Line broadening from an intrinsically narrow line emitted from two radii in an accretion disc (from Fabian et al 2000). The lowest panel show the result obtained by summing many disc radii, weighted by the expected emissivity.

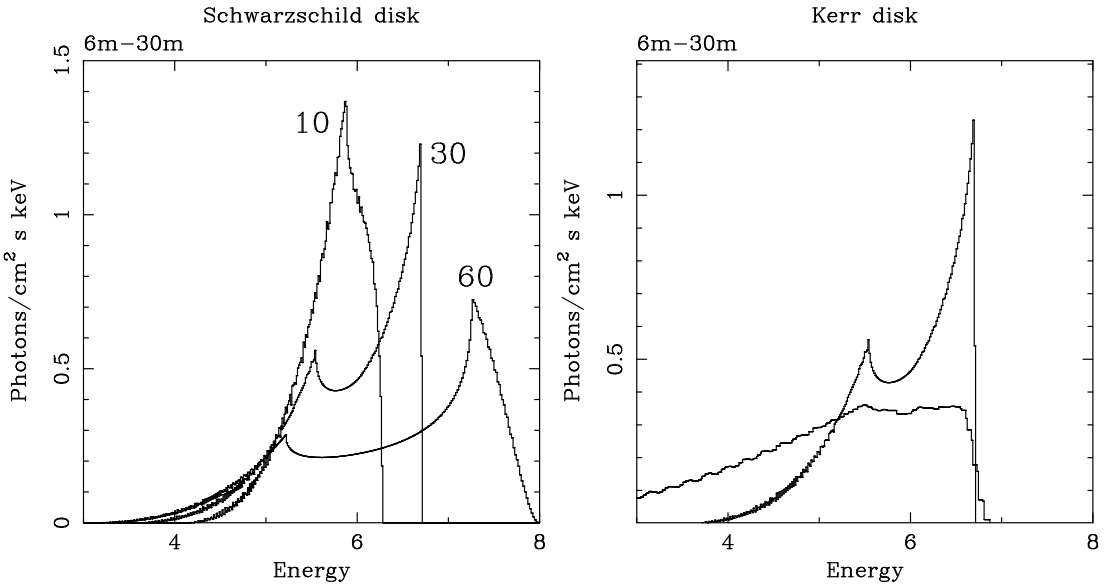

FIGURE 3. Model spectra produced by the iron Kα 6.4 keV line emitted from an accretion disc at radii (Left) $6 - 30r_g$ around a non-spinning (Fabian et al 1989) and (Right) $6 - 30r_g$ and (broader profile) $1.25 - 30r_g$ around a maximally-spinning (Laor 1990) Kerr black hole.

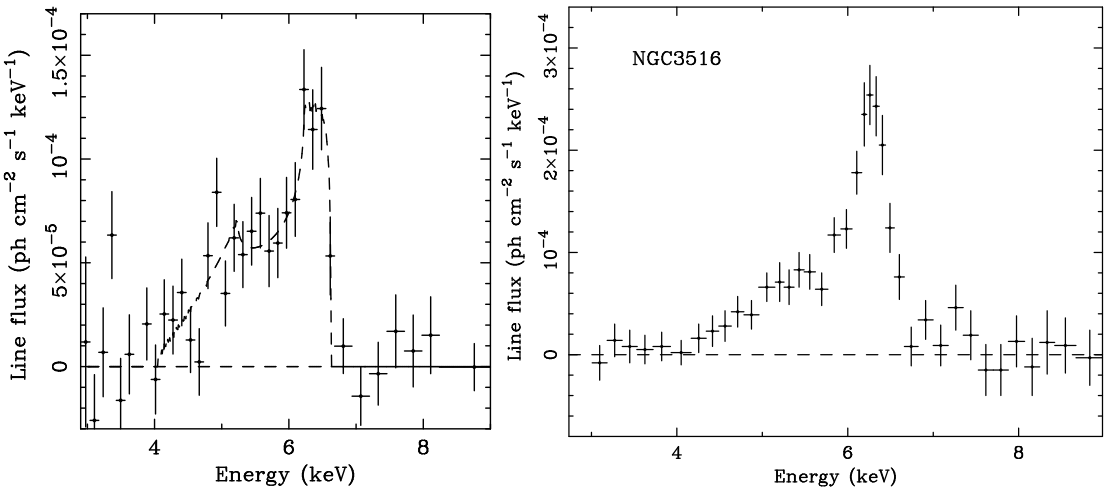

FIGURE 4. Observed profiles of broad iron lines; (Left) MCG–6-30-15 from Tanaka et al (1995) and (Right) NGC 3516 from Nandra et al (1999).

for MCG–6-30-15. A broad red wing is seen in most. Further work on the strength and width of iron lines in Seyferts is reported by Lubiński & Zdziarski (2000).

Occasionally the iron line in MCG–6-30-15 changes its profile, as in a deep minimum (Iwasawa et al 1996) or after a flare (Iwasawa et al 1999), and appears to stretch more to the red. This is possible evidence that the black hole is spinning rapidly (Iwasawa et al 1996; Dabrowski et al 1997), although matter streaming from the innermost stable orbit around a non-spinning black hole might mimic this result (Reynolds & Fabian 1997; Young et al 1998).

XMM-Newton, which has a much larger effective area than ASCA, has now observed MCG–6-30-15 and several other Seyfert 1 galaxies. The iron line profile,

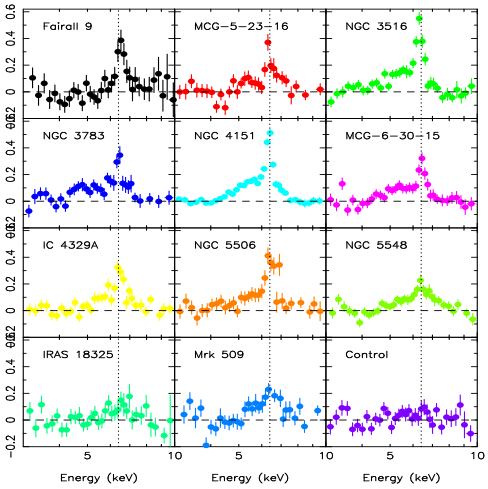

FIGURE 5. Line profiles for a selection of Seyfert 1 galaxies made by K. Nandra (prov. comm.).

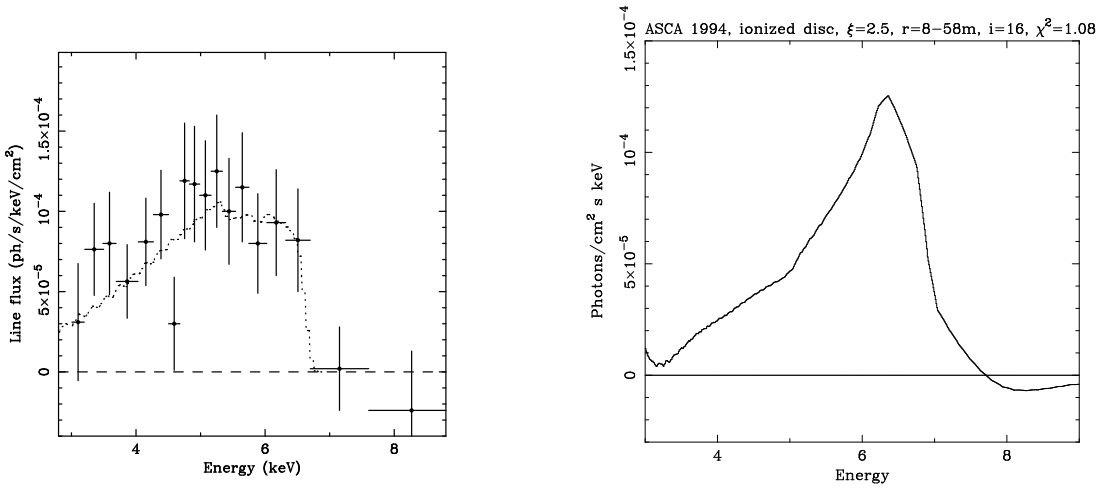

FIGURE 6. (Left) line profile druing the deep minimum of the ASCA 1994 observation (Iwasawa et al 1996). The fitted profile is for a maximal Kerr black hole. (Right) model profile for a relativistically-broadened, constant density ionized disc model fitted to the time-averaged 1994 ASCA data. Compare with Fig. 4, left panel).

kindly supplied by the PI of the observation, Joern Wilms, is shown in Fig. 8. The data in this ratio plot resemble the shape of the iron line from ASCA (Fig. 2). In the case of Mrk205 (Fig. 9) the line appears to peak around 6.7 keV, which may indicate an ionized disc (i.e. the metals have only K-shell electrons). The sharp peak at 6.4 keV may be a fluorescent line from more distant cold gas within the galaxy. Models of ionized discs have been made for constant density (e.g. Ross & Fabian 1993) and more recently for atmospheres in hydrostatic equilibrium (Nayakshin, Kazanas & Kallman 2000; Ballantyne, Ross & Fabian 2001: Fig. 7). An example of a constant density model fitted to the ASCA MCG–6-30-15 data is shown in Fig. 6. The models predict that the iron line shifts to 6.7 keV in the rest frame and oxygen and other features should be present below 1 keV. Whether these low energy features are detectable depends on their strength relative to the steep continuum.

Broad iron lines are generally not seen in objects with luminosity exceeding a few time $10^{44}\,\mathrm{erg\,s^{-1}}$ in the 2–10 keV band (Iwasawa & Taniguchi 1993; Nandra et al 1997). An example from XMM-Newton of a narrow iron line from a powerful distant quasar, PKS 0537-286, is shown in Fig. 9, from Reeves et al 2001). Narrow iron lines are expected in many AGN from reflection by outer gas at parsecs and beyond (Ghisellini et al 1994) and are seen in some Seyferts (e.g. Yaqoob et al 2000).

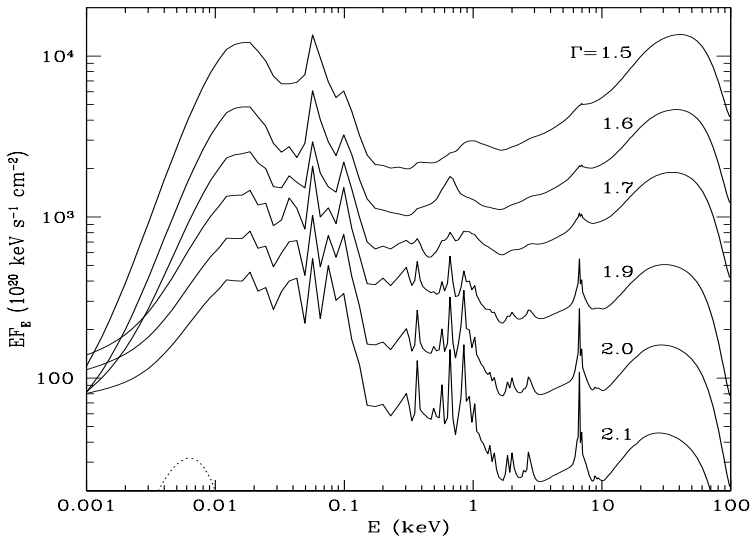

FIGURE 7. Reflection spectra from ionized accretion disc models, before relativistic blurring; see Ballantyne et al (2001) for details. The observed spectrum will usually need the addition of the power-law continuum of photon index Γ, which is not included here.

II IRON LINE VARIABILITY

The intensity of the iron line in MCG–6-30-15 does vary (Iwasawa et al 1996; 99), but not in any obvious way in response to the continuum. A long observation made simulataneously with ASCA and RXTE in 1997 (Lee et al 2000) confirms this. Vaughan & Edelson (2000) have re-analysed the RXTE data with the results shown in Fig. 10. There is real variability in the iron line flux but it is not correlated with the continuum flux. The continuum power-law slope is correlated in the sense that the spectrum steepens as the flux increases. Further work by Matsumoto et al (2000) on a 10 day ASCA observation in 1999 extends the peculiar behaviour. The RMS variability decreases towards high energy, particularly around the iron line (Fig. 11).

Various ideas have been mooted in order to explain the variability. Possibilities include; a) transrelativistic motion of flares (Reynolds & Fabian 1997; Beloborodov 1999) so that an observed bright continuum is associated with flux beamed away from the disc and vice versa (this has the problem that the spectral index trend with flux would be opposite to that observed); b) smoke from the coronal flares themselves (Merloni & Fabian in prep.) in which electron scattering in the corona smears out transmitted line emission when the regions are spatially large, and hence bright; and c) ionization variations (Lee et al 2000; Reynolds 2000).

The lack of any clear iron line – continuum correlation so far suggest that iron line reverberation (Reynolds et al 1999) may be complicated.

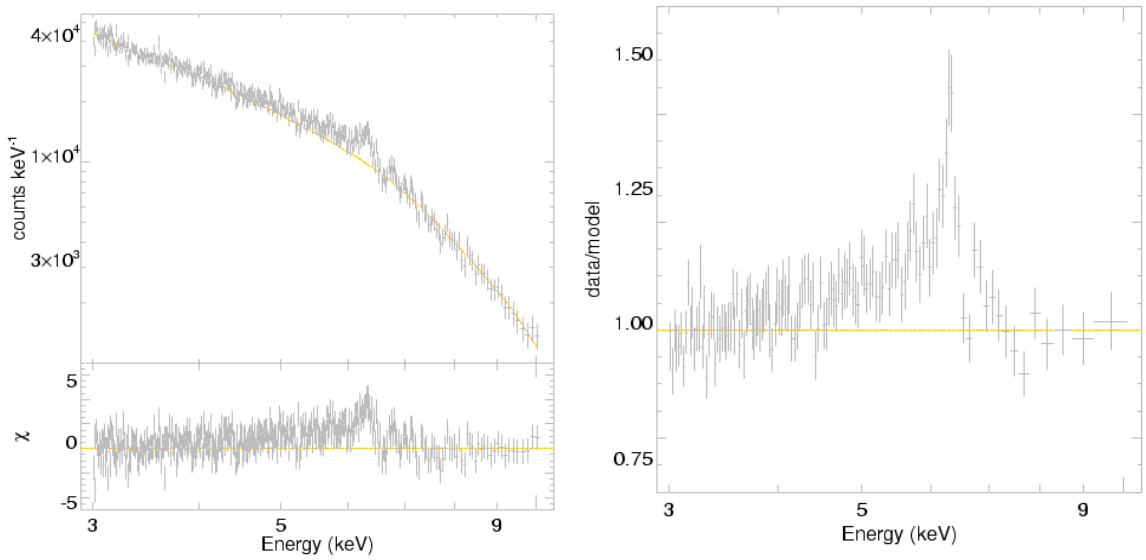

FIGURE 8. XMM-Newton EPIC-pn spectra of MCG–6-30-15. The left panel shows the whole spectrum from 3–10 keV and the right panel shows the ratio between the data and a simple power-law fitted only to the data from 3–4 and 8–10 keV. Note that the ratio plot must be multiplied by the power-law spectrum to produce a line intensity plot such as in Fig. 4.

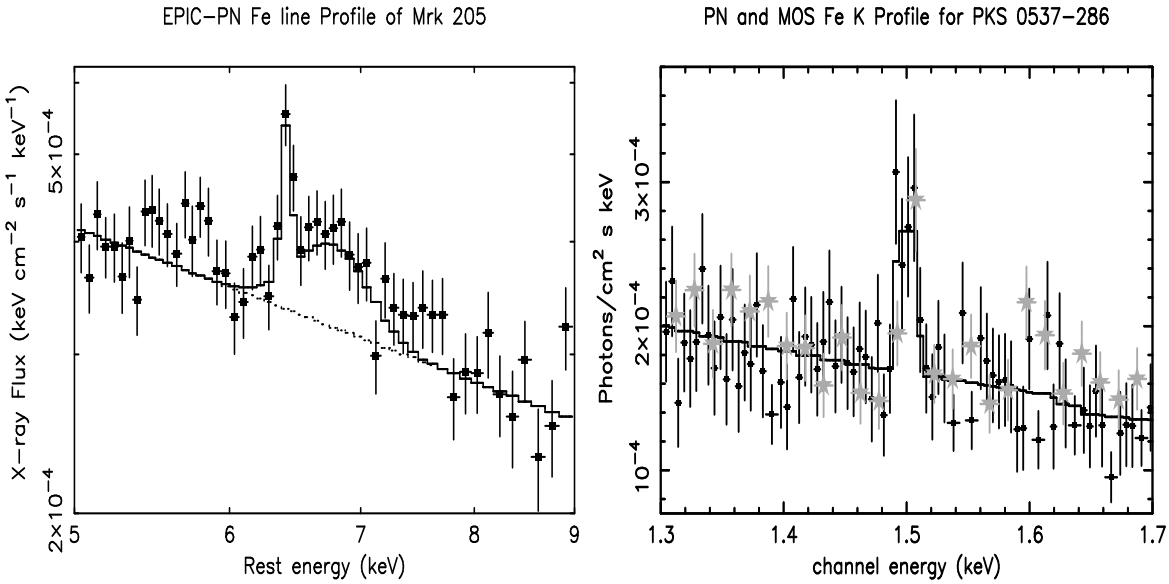

FIGURE 9. EPIC-pn spectra of the Seyfert 1 galaxy Mrk 205 (left) and the $z = 3.104$ quasar PKS 0537-286 (right), from Reeves et al (2001a,b).

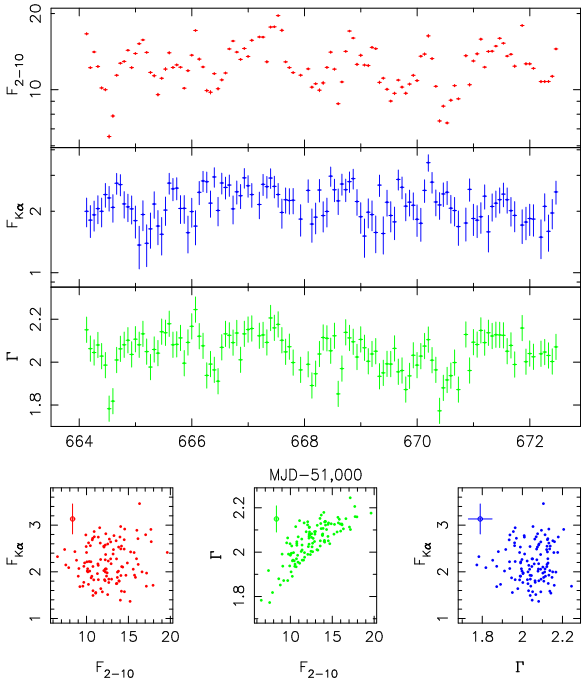

FIGURE 10. Light curves of the total 2–10 keV band flux (top), iron K-α flux (middle) and photon index (bottom) during the 1997 RXTE observation of MCG–6-30-15, from Vaughan & Edelson (2000). The lower panels show that there is no correlation between $F_{\mathrm{K}\alpha}$ and F_{2-10}.

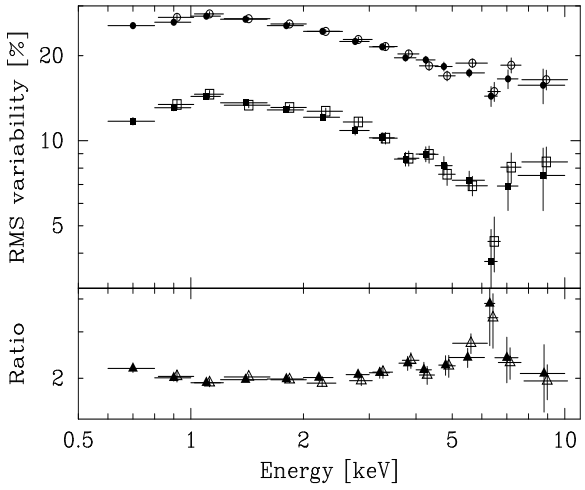

FIGURE 11. The energy dependence of the RMS variability of MCG–6-30-15, as observed with ASCA (from Matsumoto et al (2000). The 2 plots in the top panel refer to time bins of (upper) 2×10^4 s and (lower) 2×10^5 s.

III BROAD OXYGEN LINES?

A recent development has been the observation of Seyfert galaxies at high spectral resolution, provided by the gratings on Chandra and XMM-Newton. Branduardi-Raymont et al (2001) claim from XMM-Newton RGS spectra of MCG–6-30-15 the presence of relativistically-broadened oxygen, nitrogen and carbon lines. As already noted, emission lines from these elements are expected from an ionized disc. The surprise is that they might be so strong. Moreover, the spectrum of the source below 2 keV has been previously well modelled by a variable warm absorber (Fabian et al 1994; Otani et al 1996). In their original paper, Branduardi-Raymont et al (2001) rely on some unspecified mechanism for the observed spectral turndown below 2 keV and argue from the weak, broad ($2000\,\mathrm{km\,s^{-1}}$) absorption lines seen in their spectra that the column density of any warm absorber is too low to provide an edge large enough to account for the spectral jump at $\sim 0.7\,\mathrm{keV}$ (Fig. 12), moreover the jump occurs in the wrong place, requiring a redshift of $16,000\,\mathrm{km\,s^{-1}}$.

Chandra HETG spectra provide a different view of the same object (Lee et al 2001; Fig. 13). The 3 times higher spectral resolution shows that the linewidths are $< 200\,\mathrm{km\,s^{-1}}$ and, from curve of growth analysis of the OVII line series, argues for the presence of a significant warm absorber. Part of the redshift of the OVII photoelectric edge is then accounted for by the convergence of the OVII absorption line series.

The poster paper on the XMM-Newton RGS spectrum by Sako et al (2001; these proceedings) now includes a warm absorber, together with relativistically-broadened hydrogenic, C, N and O lines. Absorption by neutral iron is suspected to be a further important ingredient by the Chandra team. The neutral iron presumably being in the form of dust, which must be present to explain the high optical/UV reddening seen in the object (Reynolds et al 1997).

Since the conference, Lee et al (2001) have accounted for a major feature around the OVII edge in terms of neutral iron absorption. Of the three edges of iron-L, known as L3, L2 and L1, the absorption near threshold of Fe L3 is a deep trough in laboratory data (Kortright & Kim 2000) and in the spectrum of Cyg X-1 (Schulz et al 2001). This trough exactly matches the broad absorption feature seen in the Chandra spectrum of MCG–6-30-15 at 0.71 keV (Fig. 13) and accounts for the apparent redshift of the OVII edge (Fig. 12). Fe L2 and OVII absorption together explain the remaining features between 0.7 and 0.75 keV.

Much more detailed modelling is required, covering a wider spectral band, but it is now clear that MCG–6-30-15 does have a significant dusty warm absorber. It is plausible that there is in addition some emission from ionized C, N and O within the disc, but debatable as to whether it is strong enough to create detectable features. The relativistic line broadening parameters quoted by Branduardi-Raymont et al (2001) do not yet agree with those found for the time-averaged ASCA spectra. The ASCA results (Fig. 4) appear to be in accord with the XMM-Newton EPIC data (Fig. 8) taken simultaneously with the RGS spectra.

The Chandra spectrum does not show two spectral jumps, one of which can

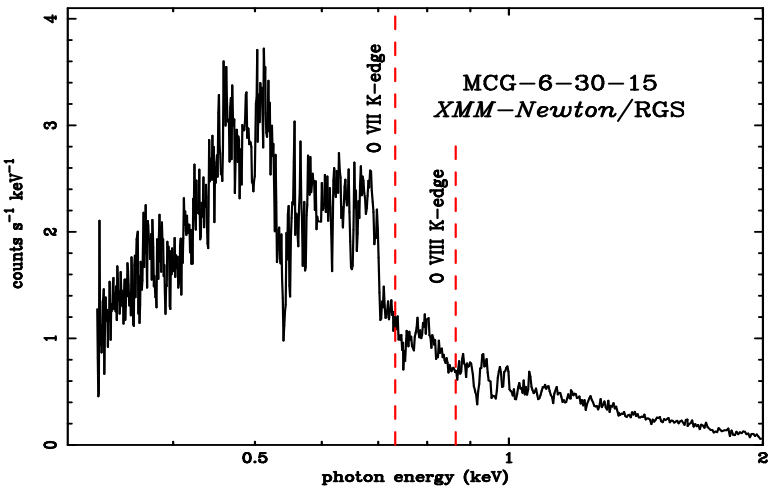

FIGURE 12. XMM-Newton RGS spectrum of MCG–6-30-15. The positions of the OVIII and OVII photoelectric absorption edges are marked (see Branduardi-Raymont et al (2001).

be explained by photoelectric absorption and the other by the blue wing of an emission line. I conclude that the large spectral jump seen around 0.7 keV is dominated by absorption features from a dusty warm absorber. Whether relativistically-broadened emission features are also present remains to be seen.

IV SUMMARY

The broad iron lines seen in MCG–6-30-15 and NGC 3516 are well explained by X-ray irradiation of an accretion disc extending very close to a black hole. The skewed shape of the lines is mainly due to the strong gravitational redshift in this region.

The variability of the iron line and the lack of correlation with continuum variations is not understood. The emission region is plausibly complex with ionization, bulk motion and scattering effects likely.

The case for a broad oxygen line in MCG–6-30-15 is unclear.

V ACKNOWLEDGEMENTS

I thank David Ballantyne, Claude Canizares, Kazushi Iwasawa, Julia Lee, Raquel Morales, Patrick Ogle, Randy Ross, Norbert Schulz and Simon Vaughan for help and Chiho Matsumoto, Paul Nandra, James Reeves, Masao Sako and Joern Wilms for sending me plots in advance of publication.

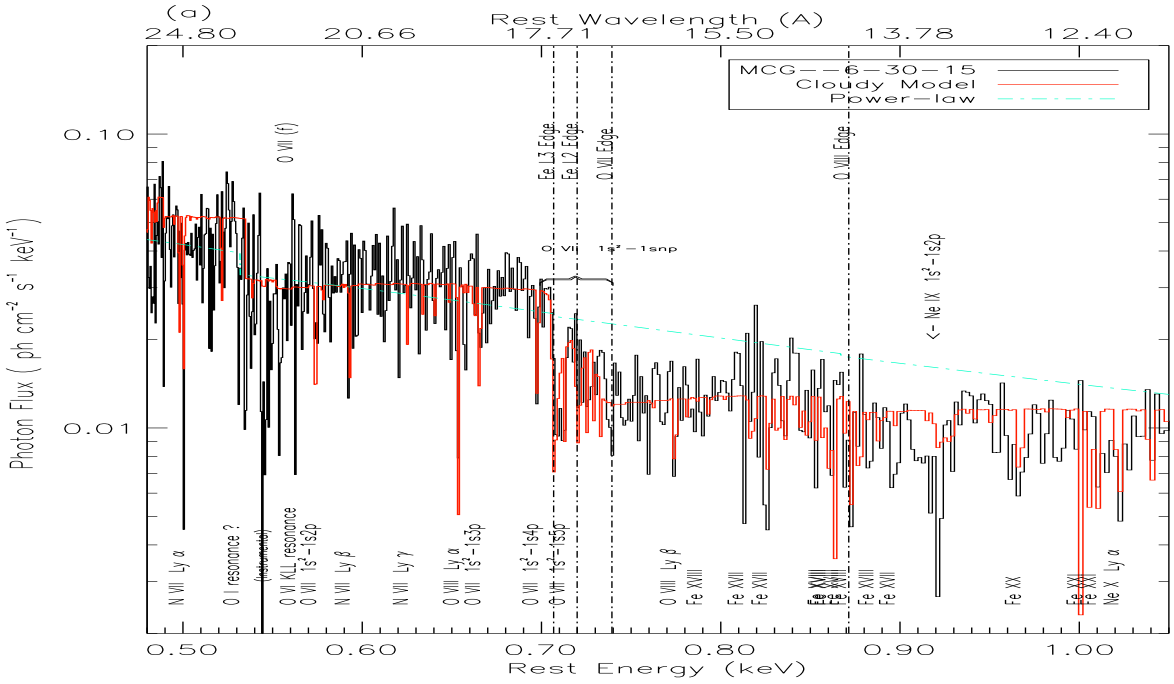

FIGURE 13. Chandra HETG spectrum of MCG–6-30-15 (Lee et al 2001). The CLOUDY model fit includes absorption due to neutral Fe-L assumed to arise from dust in the source.The large trough centred at 0.71 keV is due to Fe-L3 absorption.

REFERENCES

Ballantyne D.R., Ross R.R., Fabian A.C., 2001, MNRAS in press, (astro-ph/0102268)

Beloborodov A., 1999, ApJ, 510, 123

Branduardi-Raymont G., M. Sako, S.M. Kahn, Brinkman A.C., Kaastra J.S., Page M.J., 2001, A&A, 365, L140

Dabrowski, Y. et al., 1997, MNRAS, 288, L11

Eckart A., Genzel R., 1997, MNRAS, 284, 576

Fabian A.C., et al 1994, PASP, 46, L59

Fabian A.C., Nandra K., Reynolds C.S., Brandt W.N., Otani C., Tanaka Y., Inoue H., Iwasawa K., 1995, MNRAS, 277, L11

Fabian A.C., Rees M.J., Stella L., White N.E., 1989, MNRAS, 238,729

Fabian A.C., Reynolds C.S., Iwasawa K., Young A., 2000, PASP, 112,1145

Ferrarese L., Merritt D., 2000, ApJ, 539, L9

Gebhardt K., 2000, ApJ, 539, L13

George I.M., Fabian A.C., 1991, MNRAS, 249, 352

Ghez A.M., Morris M., Becklin E.E., Tanner A., Kremenek T., 2000, Nature 407, 349

Ghisellini G., Haardt F., Matt G., 1994, MNRAS, 267, 743

Iwasawa K., Taniguchi Y., 1993, ApJ, 413, L15

Iwasawa, K. et al., 1996, MNRAS, 282, 1038

Iwasawa K., Fabian A.C., Young A., Matsumoto C., Inoue C., 1999, MNRAS, 306, L19

Kortright J.B., Kim S.K., 2000, Phys Rev. B, 12216
Laor, A., 1991, ApJ, 376, 90
Lee J., Fabian A. C., Reynolds C. S., Brandt W. N., Iwasawa K., 2000, MNRAS, 318, 857
Lee J., Ogle P.M., Canizares C.S., Marshall H.L., Schulz N.S., Morales R.M., Fabian A. C., Iwasawa K., 2001, ApJ, submitted (astro-ph/0101065)
Matt, G., Perola, G.C., Piro L., 1991, AaA, 247, 25
Miyoshi M., et al 1995, Nature, 373, 127
Nandra K., George I.M., Mushotzky R.F., Turner T.J., Yaqoob Y., 1997, ApJ, 488, 91
Nandra K., George I. M., Mushotzky R. F., Turner T. J., Yaqoob T., 1999, ApJ, 523, L17
Nayaksin S., Kazanas D., Kallman T. R., 2000, ApJ, 537, 833
Otani C. et al., 1996, PASJ, 48, 211
Reeves J.N., et al 2001a, A&A, 365, L116
Reeves J.N., et al 2001a, A&A, 365, L134
Reynolds C. S., 2000, ApJ, 533, 811
Reynolds, C.S., Ward, M.J., Fabian A.C., Celotti A., 1997, MNRAS, 291, 403
Reynolds, C.S., Begelman, M.C., 1997, ApJ, 488, 109
Reynolds, C.S. Young A.J., Begelman M.C., Fabian A.C., 1998, ApJ, 514, 164
Ross, R.R., Fabian, A.C., 1993, MNRAS, 261, 74
Schulz N.S., et al 2001, in preparation
Tanaka, Y. et al., 1995, Nature, 375, 659
Vaughan S., Edelson R. 2000, ApJ, 548, 694
Yaqoob T., George I. M., Nandra K., Turner T. J., Serlemitsos P. J., Mushotzky R.F., 2000, ApJ, 546, 759
Lubiński P., Zdziarski A.A., 2001, MNRAS, in press (astro-ph/0009017)